Eur. Phys. J. Plus (2015) **130**: 100
DOI 10.1140/epjp/i2015-15100-y

THE EUROPEAN PHYSICAL JOURNAL PLUS

Regular Article

Effect of thermal radiation on velocity and temperature fields of a thin liquid film over a stretching sheet in a porous medium

M. Darzi[1], M. Vatani[2], S.E. Ghasemi[3,a], and D.D. Ganji[2]

[1] Department of Mechanical Engineering, College of Engineering, University of Tehran, Tehran, Iran
[2] Department of Mechanical Engineering, Babol University of Technology, Babol, Iran
[3] Young Researchers and Elite Club, Qaemshahr Branch, Islamic Azad University, Qaemshahr, Iran

Received: 2 March 2015 / Revised: 4 April 2015
Published online: 29 May 2015 –

Abstract. An analytical approach using the least-squares method (LSM) has been carried out to study the effect of thermal radiation on the flow and heat transfer in a thin liquid film over an unsteady stretching sheet embedded in a porous medium. Similarity transformations were used to convert the momentum, continuity and energy equations describing the problem, which are coupled nonlinear partial differential equations into a set of nonlinear ordinary differential equations. The resulting set of Ordinary Differential Equation (ODE) is then solved analytically by the least-squares method. By comparing the results of the applied method with previously published work the accuracy of the proposed method has been verified. Finally the effects of different outstanding parameters in this particular case such as the Darcy parameter, the radiation parameter and the Prandtl number on the flow velocity and temperature profiles are communicated.

1 Introduction

Recently investigations on the concept of porous media are attracting much more attention due to its vast applications in nowadays industry. One can easily observe the significant role of porous media in various engineering problems such as geomechanics, petroleum engineering, material science, and acoustics. Plenty of studies have been carried out in fluid flow and heat transfer through porous media. Cheng and Minkowycz [1] and also Cheng [2] studied the natural convection over a vertical impermeable flat plate in a saturated porous medium. Ramanaiah [3] studied non-Darcy axisymmetric free convection on permeable horizontal surfaces in a saturated porous medium. Hooper *et al.* [4] studied the subject of mixed convection from an isothermal vertical plate in porous media with uniform surface suction or injection. Wright *et al.* [5] performed a theoretical and numerical investigation on the natural convection about a vertical plate with a prescribed surface heat flux in porous medium. Yih [6] numerically analyzed the effect of uniform lateral mass flux on heat transfer characteristics in free convection over a cone subjected to uniform wall temperature or uniform heat flux, embedded in a saturated porous medium. Gorla and Takhar [7] focused on mixed convection along a vertical plate with surface mass transfer. They investigated the effect of suction and injection on mixed convection in non-Newtonian fluids in porous media. Chin *et al.* [8] studied the effect of variable viscosity on mixed convection boundary layer flow over a vertical impermeable surface embedded in a porous medium. Rashad *et al.* [9] studied the mixed convection flow of non-Newtonian fluid from vertical surface saturated in a porous medium filled with nanofluids.

The fluid flow and heat transfer of a thin liquid film over a stretching sheet is an important phenomenon in understanding the coating process and design of various heat exchangers, chemical processing equipment, reactor fluidization, transpiration cooling and etc. In a melt-spinning process, the extrudate from the die is generally drawn and simultaneously stretched into a filament or sheet, which is then solidified through rapid quenching or gradual cooling by direct contact with water or chilled metal rolls. In fact, stretching imparts a unidirectional orientation to the extrudate, thereby improving its mechanical properties as the quality of the final product greatly depends on the rate of cooling. Crane [10] first studied the steady two-dimensional boundary layer flow induced by the stretching

[a] e-mail: s.ebrahim.ghasemi@gmail.com

of an elastic flat sheet in its own plane with a velocity which varies linearly with the distance from a fixed point on the sheet and gave an exact similarity solution. This work subsequently received considerable attention by many researchers due to its practical applications. Literature contains several studies about stretching sheet flow problem either by considering the effects of rotation, heat and mass transfer, chemical reaction, MHD, non-Newtonian fluid or different possible combinations of these above effects [11–17].

In all these studies, the boundary layer equation is considered and the boundary conditions are prescribed at the sheet and on the fluid outside the boundary layer at infinity. Imposition of similarity transformation reduces the system to a set of ODEs, which are then solved either analytically or numerically. Wang [18] first studied the flow of a thin liquid film over an unsteady stretching sheet. In this study, he used a special type of similarity transformation to reduce the boundary layer equations into a set of nonlinear ODE and then solved numerically. Using this special type of similarity transformation, Andersson *et al.* [19,20] and Chen [21] extended the study of unsteady stretching sheet flow of a liquid film to the case of power law fluid, heat transfer. Liu and Andersson [22] extended the problem considered by Andersson *et al.* [20] in the case of a more general form of the prescribed surface temperature variation. Dandapat *et al.* [23] studied the effects of thermocapillarity on the flow of a thin liquid film over an unsteady stretching sheet. Wang [24] presented exact analytical solutions for the momentum and heat transfer within an unsteady thin liquid film over a stretching sheet. Noor and Hashim [25] investigated the effects of thermocapillarity and of a magnetic field in a thin liquid film on an unsteady elastic stretching sheet. Khader and Megahed [26] presented a numerical simulation of the flow and heat transfer in a thin liquid film over an unsteady stretching sheet in a saturated porous medium in the presence of thermal radiation by using the finite-difference method. Recently Mairy [27] investigated the flow and heat transfer of a thin liquid film over an unsteady porous stretching sheet in the presence of suction or injection by considering a full set of momentum equations.

Lots of equations in the fluid flow and heat transfer problems have a nonlinearity form and should be solved by analytical and numerical approaches. There are some simple and accurate analytical techniques for solving nonlinear differential equations called the Weighted Residuals Methods (WRMs). The collocation method, the Galerkin method and the least-square method (LSM) are examples of the WRMs that are introduced by Ozisik [28] for using in the heat transfer problems. Stern and Rasmussen [29] used the collocation method for solving a third-order linear differential equation. Vaferi *et al.* [30] have studied the feasibility of applying the Orthogonal Collocation method to solve the diffusivity equation in the radial transient flow system. Hatami *et al.* [31] used LSM for the heat transfer problem through porous fins, and also the problem of a laminar nanofluid flow in a semi-porous channel in the presence of transverse magnetic field has been investigated analytically by Sheikholeslami *et al.* [32] which used LSM. Moreover, LSM is introduced by Aziz and Bouaziz [33,34] for predicting the performance of longitudinal fins. They found that the least-squares method is simple compared with other analytical methods. Shaoqin and Huoyuan [35] developed and analyzed least-squares approximations for the incompressible magneto-hydrodynamic equations. Hatami and Ganji [36] found that LSM is more appropriate than other analytical methods for solving the nonlinear heat transfer equations. Hatami *et al.* [37] investigated the heat transfer and fluid flow mechanism for a Cu-water (water with copper nanoparticles) nanofluid cooled microchannel by porous media approach. They introduced and solved the temperature distribution in both solid (fin) and fluid (Cu-water) phases by the Least-Squares Method.

Flow analysis for a third grade non-Newtonian blood in porous arteries in the presence of magnetic field was simulated analytically and numerically by Ghasemi *et al.* [38]. They used the Collocation Method (CM) and the Optimal Homotopy Asymptotic Method (OHAM) to solve the Partial Differential Equation (PDE) governing equation, and a good agreement between the two methods was observed in their results.

Ghasemi *et al.* [39] applied the Optimal Homotopy Asymptotic Method (OHAM) and the Homotopy Perturbation Method (HPM) to obtain the temperature distribution in a flat-plate air-heating solar collector.

Also, Ghasemi *et al.* [40,41] applied the Differential Transformation Method (DTM) to analyze the temperature distribution in solid and porous fins with temperature-dependent heat generation and thermal conductivity.

Steady, laminar, incompressible and two-dimensional micropolar flow between a porous disk and a nonporous disk was investigated using the Optimal Homotopy Asymptotic Method (OHAM) by Vatani *et al.* [42].

Recently, the motion of a spherical particle released in a swirling fluid flow was studied employing the least-squares method and the method of moments by Ghasemi *et al.* [43].

Electrohydrodynamic flow (EHD flow) in a circular cylindrical conduit was studied using the Least-Squares Method (LSM) by Ghasemi *et al.* [44]. They concluded that LSM is in excellent agreement with the numerical solution, also depicted residual functions showed that LSM is more acceptable than the Homotopy Analysis Method (HAM).

The main aim of this paper is the application of the Least-Squares Method (LSM) to simulate the problem of flow and heat transfer in a thin liquid film over an unsteady stretching sheet in a saturated porous medium in the presence of thermal radiation. So the novelty of this study is the utilization of LSM as a powerful and efficient technique for solving the nonlinear equations of thermal radiation on the velocity and temperature fields of a thin liquid film over an unsteady stretching sheet embedded in a porous medium.

Furthermore, the accuracy and effectiveness of the proposed method is compared and comprehensively discussed.

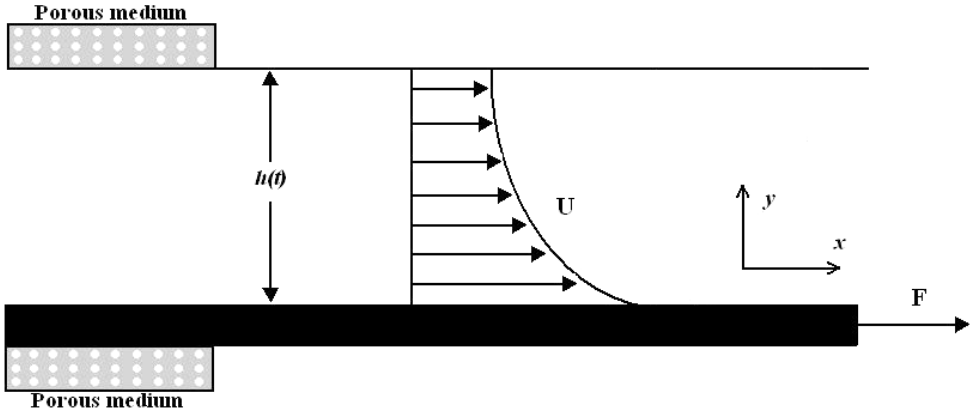

Fig. 1. Schematic of the problem.

2 Problem description and governing equations

Suppose the unsteady flow of a Newtonian fluid in a thin liquid film over a stretching surface, which is pulled with the force F. The elastic sheet issues from a narrow slit at the origin of a Cartesian coordinate system and the continuous surface aligned with the x-axis at $y = 0$ moves in its own plane with a velocity $U(x,t)$ and temperature distribution $T_s(x,t)$. A thin liquid film of uniform thickness $h(t)$ lies on the horizontal surface. The general schematic of the physical system is shown in fig. 1. The governing flow and heat transfer equations ruled in the boundary layer are as follows:

$$\frac{\partial u}{\partial x} + \frac{\partial \upsilon}{\partial y} = 0, \tag{1}$$

$$\frac{\partial u}{\partial t} + u\frac{\partial u}{\partial x} + \upsilon\frac{\partial u}{\partial y} = \frac{\mu}{\rho}\frac{\partial^2 u}{\partial y^2} - \frac{\mu}{\rho K}u, \tag{2}$$

$$\frac{\partial T}{\partial t} + u\frac{\partial T}{\partial x} + \upsilon\frac{\partial T}{\partial y} = \frac{\kappa}{\rho c_p}\frac{\partial^2 T}{\partial y^2} - \frac{1}{\rho c_p}\frac{\partial q_r}{\partial y}, \tag{3}$$

where u and υ are the velocity components along the x and y directions, respectively. K is the permeability of the porous medium, κ is the thermal conductivity, ρ is the fluid density, t is the time, T is the temperature of the fluid, q_r is the radiative heat flux, μ is the viscosity of the fluid and c_p is the specific heat at constant pressure.

The suitable boundary conditions for this problem are

$$u = U, \qquad \upsilon = 0, \qquad T = T_s \quad \text{at} \quad y = 0, \tag{4}$$

$$\frac{\partial u}{\partial y} = \frac{\partial T}{\partial y} = 0, \quad \text{at} \quad y = h, \tag{5}$$

$$\upsilon = \frac{\mathrm{d}h}{\mathrm{d}t}, \quad \text{at} \quad y = h, \tag{6}$$

where U is the surface velocity of the stretching sheet and the flow is caused by stretching the elastic surface at $y = 0$ such that continuous sheet moves in the x-direction with the velocity

$$U = \frac{bx}{1 - at}, \tag{7}$$

where h is the thickness of the liquid film. a and b are the positive constants with dimension $(time)^{-1}$. T_s is the surface temperature of the stretching sheet varies with the distance x along the sheet and time t in the form

$$T_s = T_0 - T_{ref}\left(\frac{bx^2}{2(\mu/\rho)}\right)(1 - at)^{-\frac{3}{2}}, \tag{8}$$

where T_0 is the temperature at the slit and T_{ref} is the constant reference temperature for all $t < \frac{1}{a}$.

The radiative heat flux q_r is employed according to Rosseland approximation [45] such that

$$q_r = -\frac{4\sigma^*}{3k^*}\frac{\partial T^4}{\partial y}, \tag{9}$$

where σ^* is the Stefan-Boltzmann constant and k^* is the mean absorption coefficient. Following Rapits [46], we assume that the temperature differences within the flow are small such that may be expressed as a linear function of the temperature. Expanding T^4 in a Taylor series about T_0 and neglecting higher-order terms, we have

$$T^4 \cong 4T_0^3 T - 3T_0^4. \tag{10}$$

The special form of the surface velocity (7) and the surface temperature (8) allow the system of partial differential eqs. (2) and (3) to be transformed to a system of coupled nonlinear ordinary differential equations by using the following similarity transformations [25]:

$$\eta = \left(\frac{b}{(\mu/\rho)}\right)^{\frac{1}{2}} (1-at)^{-\frac{1}{2}}\beta^{-1} y, \tag{11}$$

$$u = bx(1-at)^{-1} f'(\eta), \tag{12}$$

$$\upsilon = -\left(\frac{\mu b}{\rho}\right)^{\frac{1}{2}} (1-at)^{-\frac{1}{2}}\beta f(\eta), \tag{13}$$

$$T = T_0 - T_{ref}\left(\frac{bx^2}{2(\mu/\rho)}\right)(1-at)^{-\frac{3}{2}}\theta, \tag{14}$$

where β is yet an unknown constant denoting the dimensionless thin film thickness, defined by Noor and Hashim [25]:

$$\beta = \left(\frac{b}{(\mu/\rho)}\right)^{\frac{1}{2}} (1-at)^{\frac{-1}{2}} h(t), \tag{15}$$

Using eqs. (11)–(14), the mathematical problem defined in eqs. (1)–(3) are then transformed into the following set of ordinary differential equations:

$$f''' + \gamma\left[ff'' - \frac{S}{2}\eta f'' - f'^2 - (S+D)f'\right] = 0, \tag{16}$$

$$\frac{1}{Pr}\left[(1+R)\theta''\right] + \gamma\left[f\theta' - 2f'\theta - \frac{S}{2}\eta\theta' - \frac{3}{2}S\theta\right] = 0, \tag{17}$$

subject to the boundary conditions

$$f(0) = 0, \qquad f'(0) = 1, \qquad ,\theta(0) = 1, \tag{18}$$

$$f''(1) = 0, \qquad \theta'(1) = 0, \tag{19}$$

$$f(1) = \frac{1}{2}S, \tag{20}$$

where primes denote differentiation with respect to η, $S = \frac{a}{b}$ is the unsteadiness parameter, $Pr = \frac{\mu c_p}{\kappa}$ is the Prandtl number, $\gamma = \beta^2$ is the dimensionless film thickness, $R = \frac{16\sigma^* T_0^3}{3k^*\kappa}$ is the radiation parameter and $D = \frac{\mu(1-at)}{\rho b k}$ is the Darcy number.

The physical quantities of interest are the skin-friction coefficient C_f and the local Nusselt number Nu_x which are defined as

$$C_f = \frac{2}{\beta} f''(0) Re_x^{\frac{-1}{2}}, \tag{21}$$

$$Nu_x = \frac{1}{2\beta(1-at)^{\frac{1}{2}}}\theta'(0) Re_x^{\frac{3}{2}}, \tag{22}$$

where $Re_x = \frac{\rho U x}{\mu}$ is the local Reynolds number.

3 Applied analytical method

3.1 Least-Square Method (LSM)

The least-square method is one of the estimation techniques for solving differential equations called the Weighted Residual Methods (WRMs) which firstly introduced by Ozisik [28] to solve nonlinear equations arising from heat transfer problems. For conception the main idea of this method, consider a differential operator D is performed on a function u to produce a function p [34]:

$$D(u(x)) = p(x). \tag{23}$$

It is supposed that u is approximated by a function $\tilde{u}$, which is a linear combination of basic functions chosen from a linearly independent set. That is

$$u \cong \tilde{u} = \sum_{i=1}^{n} c_i \varphi_i. \tag{24}$$

Now, when substituted into the differential operator, D, the result of the operations generally is not $p(x)$. Hence an error or residual will exist:

$$R(x) = D(\tilde{u}(x)) - p(x) \neq 0. \tag{25}$$

The notion in WRMs is to force the residual to zero in some average sense over the domain. That is

$$\int_x R(x) W_i(x) = 0 \qquad i = 1, 2, \ldots, n, \tag{26}$$

where the number of weight functions W_i is exactly equal the number of undefined constants c_i in $\tilde{u}$. The result is a set of n algebraic equations for the unknown coefficients c_i. If the continuous summation of all the squared residuals is minimized, the reasoning behind the LSM name can be seen. In other words, a minimum of

$$S = \int_x R(x) R(x) \mathrm{d}x = \int_x R(x)^2 \mathrm{d}x. \tag{27}$$

In order to achieve a minimum of this scalar function, the derivatives of S with respect to all the unknown parameters must be zero. That is

$$\frac{\partial S}{\partial c_i} = 2 \int_x R(x) \frac{\partial R}{\partial c_i} \mathrm{d}x = 0. \tag{28}$$

Comparing with eq. (26), the weight functions are seen to be

$$W_i = 2 \frac{\partial R}{\partial c_i}. \tag{29}$$

However, the "2" coefficient can be dropped, since it cancels out in the equation. Therefore the weight functions for the least squares method are just the derivatives of the residual with respect to the unknown constants [36] as follows:

$$W_i = \frac{\partial R}{\partial c_i}. \tag{30}$$

Many advantages of LSM compared to other analytical and numerical methods make it more valuable and motivate researchers to use it for solving heat transfer problems. Some of these advantages are listed below [36]:

a) It solves the equations directly and no simplifications are needed.
b) It does not need any perturbation, linearization or small parameter with respect to the Homotopy Perturbation Method (HPM) and the Parameter Perturbation Method (PPM).
c) It is simple and powerful compared to numerical methods and reaches final results faster than numerical procedures while its results are acceptable and have excellent agreement with numerical outcomes. Furthermore, increasing the statements of the trial functions leads to enhancing the accuracy of the results.
d) It does not need to determine the auxiliary parameter and auxiliary the function with respect to the Homotopy Analysis Method (HAM).

More information about the accuracy of these methods in solving the nonlinear problems is presented in [31,36].

3.2 Solution procedure using LSM

The main purpose of this study is to solve the problem (16)-(17) with the boundary conditions (18)-(20) by applying the least square method. For solving eqs. (16)-(17), trial functions must satisfy the boundary conditions. So, they will be considered as

$$f(\eta) = S\frac{\eta}{2} + c_1\eta(1-\eta) + c_2\eta^2(1-\eta) + c_3\eta^3(1-\eta), \tag{31}$$

$$v(\eta) = 1 + c_4\left(\eta - \frac{\eta^2}{2}\right) + c_5\left(\eta - \frac{\eta^3}{3}\right) + c_6\left(\eta - \frac{\eta^4}{4}\right), \tag{32}$$

$$\theta(\eta) = 1 + c_7\left(\eta - \frac{\eta^2}{2}\right) + c_8\left(\eta - \frac{\eta^3}{3}\right) + c_9\left(\eta - \frac{\eta^4}{4}\right). \tag{33}$$

In this problem, we have three coupled equations. So three residual functions will be obtained as follows:

$$R_1(c_1 - c_9, \eta) = \frac{1}{2}S + c_1(1-\eta) - c_1\eta + 2c_2\eta(1-\eta) - c_2\eta^2 + 3c_3\eta^2(1-\eta) - c_3\eta^3 - 1 - c_4\left(\eta - \frac{1}{2}\eta^2\right)$$

$$- c_5\left(\eta - \frac{1}{3}\eta^3\right) - c_6\left(\eta - \frac{1}{4}\eta^4\right) \tag{34}$$

$$R_2(c_1 - c_9, \eta) = -c_4 - 2c_5\eta - 3c_6\eta^2 + \gamma\left(\left(\frac{1}{2}S\eta + c_1\eta(1-\eta) + c_2\eta^2(1-\eta) + c_3\eta^3(1-\eta)\right)(c_4(1-\eta)\right.$$

$$\left. + c_5(1-\eta^2) + c_6(1-\eta^3)\right) - \frac{1}{2}S\eta(c_4(1-\eta) + c_5(1-\eta^2) + c_6(1-\eta^3)) - \left(1 + c_4\left(\eta - \frac{1}{2}\eta^2\right)\right.$$

$$\left. + c_5\left(\eta - \frac{1}{3}\eta^3\right) + c_6\left(\eta - \frac{1}{4}\eta^4\right)\right)^2 - (S+0.2)\left(1 + c_4\left(\eta - \left(\frac{1}{2}\right)\eta^2\right) + c_5\left(\eta - \frac{1}{3}\eta^3\right) + c_6\left(\eta - \frac{1}{4}\eta^4\right)\right) \tag{35}$$

$$R_3(c_1 - c_9, \eta) = -2c_7 - 4c_8\eta - 6c_9\eta^2 + \gamma\left(\left(\frac{1}{2}S\eta + c_1\eta(1-\eta) + c_2\eta^2(1-\eta) + c_3\eta^3(1-\eta)\right)(c_7(1-\eta)\right.$$

$$\left. + c_8(1-\eta^2) + c_9(1-\eta^3)\right) - \left(2\left(1 + c_4\left(\eta - \frac{1}{2}\eta^2\right) + c_5\left(\eta - \frac{1}{3}\eta^3\right) + c_6\left(\eta - \frac{1}{4}\eta^4\right)\right)\right)\left(1 + c_7\left(\eta - \frac{1}{2}\eta^2\right)\right.$$

$$\left. + c_8\left(\eta - \frac{1}{3}\eta^3\right) + c_9\eta - \frac{1}{4}\eta^4\right)\right) - \frac{1}{2}S\eta(c_7(1-\eta) + c_8(1-\eta^2) + c_9(1-\eta^3)) - \frac{3}{2}S\left(1 + c_7\left(\eta - \frac{1}{2}\eta^2\right)\right.$$

$$\left. + c_8\left(\eta - \frac{1}{3}\eta^3\right) + c_9\left(\eta - \frac{1}{4}\eta^4\right)\right)\right). \tag{36}$$

By substituting the residual functions, $R_1(c_1 - c_9, \eta)$, $R_2(c_1 - c_9, \eta)$ and $R_3(c_1 - c_9, \eta)$, into eq. (28), a set of equations with nine equations will be obtained and by solving this system of equations, $c_1 - c_9$ coefficients will be determined. For example, by using the least-square method for this problem for the case $S = 0.8$, $Pr = 1$, $D = 0.2$, $R = 1$, $f(\eta)$, $v(\eta)$ and $\theta(\eta)$ are as follows:

$$f(\eta) = 0.4\eta + 0.62144\eta(1-\eta) - 0.69599\eta^2(1-\eta) + 0.30827\eta^3(1-\eta), \tag{37}$$

$$v(\eta) = 1 - 2.9434\eta + 4.4012\eta^2 - 3.3928\eta^3 + 1.0799\eta^4, \tag{38}$$

$$\theta(\eta) = 1 - 2.4466\eta + 3.4512\eta^2 - 2.60845\eta^3 + 0.84237\eta^4. \tag{39}$$

4 Results and discussions

In the present work, after obtaining the equations of the problem we solved them by the analytical method due to its rational nonlinearity form and discuss results. For verifying the accuracy of the present method, the results are

Table 1. Results for $f''(0)$ and $-\theta'(0)$ *versus* different values of S compared with those of Khader& Megahed [26] when $Pr = R = 1$ and $D = 0.2$.

S	$f''(0)$		$-\theta'(0)$	
	Present work (LSM)	Khader & Megahed [26]	Present work (LSM)	Khader & Megahed [26]
0.8	−2.90241	−2.90571	2.40123	2.42829
1.2	−1.43187	−1.44029	1.16875	1.18491
1.6	−0.51519	−0.51607	0.63952	0.64158

Table 2. Results for $f''(0)$ and $-\theta'(0)$ *versus* different values of D compared with those of Khader& Megahed [26] when $Pr = R = 1$ and $S = 0.8$.

D	$f''(0)$		$-\theta'(0)$	
	Present work (LSM)	Khader & Megahed [26]	Present work (LSM)	Khader & Megahed [26]
0.2	−2.90480	−2.90572	2.42571	2.42829
0.4	−2.90297	−2.90428	2.27401	2.27474
0.6	−2.90185	−2.90234	2.13986	2.14948

Table 3. Results for $f''(0)$ and $-\theta'(0)$ *versus* different values of R compared with those of Khader and Megahed [26] when $Pr = 1$, $D = 0.2$ and $S = 0.8$.

R	$f''(0)$		$-\theta'(0)$	
	Present work (LSM)	Khader & Megahed [26]	Present work (LSM)	Khader & Megahed [26]
1	−2.9055	−2.9057	2.42640	2.42829
3	−2.9053	−2.9057	1.54467	1.54551
5	−2.9051	−2.9057	0.91798	0.91955

Table 4. Results for $f''(0)$ and $-\theta'(0)$ *versus* different values of Pr compared with those of Khader& Megahed [26] when $R = 1$, $D = 0.2$ and $S = 0.8$.

Pr	$f''(0)$		$-\theta'(0)$	
	Present work (LSM)	Khader & Megahed [26]	Present work (LSM)	Khader & Megahed [26]
1	−2.9055	−2.9057	2.42803	2.42829
2	−2.9050	−2.9057	3.60835	3.60876
3	−2.9056	−2.9057	4.45348	4.45389

compared with those obtained numerically by Khader and Megahed [26]. The variations of the skin-friction coefficient in term of $f''(0)$ and the local Nusselt number in terms of $-\theta'(0)$ for different values of governing parameters are presented in tables 1–4 and as can be seen from the tables, excellent agreement is achieved. According to table 1 the value of the skin-friction coefficient $f''(0)$ increases with the unsteadiness parameter S and the reverse is true for the local Nusselt number $-\theta'(0)$. The similar behavior is also observed for the Darcy parameter in table 2. From table 3, it is concluded that by increasing the radiation parameter R, the value of local Nusselt number $-\theta'(0)$ decreases. However, the value of the skin-friction coefficient $f''(0)$ is almost constant. In addition, table 4 presents the same characteristics for the Prandtl number. As is seen, the heat flux $-\theta'(0)$ increases with the Prandtl number Pr and again the skin-friction coefficient $f''(0)$ never changes significantly.

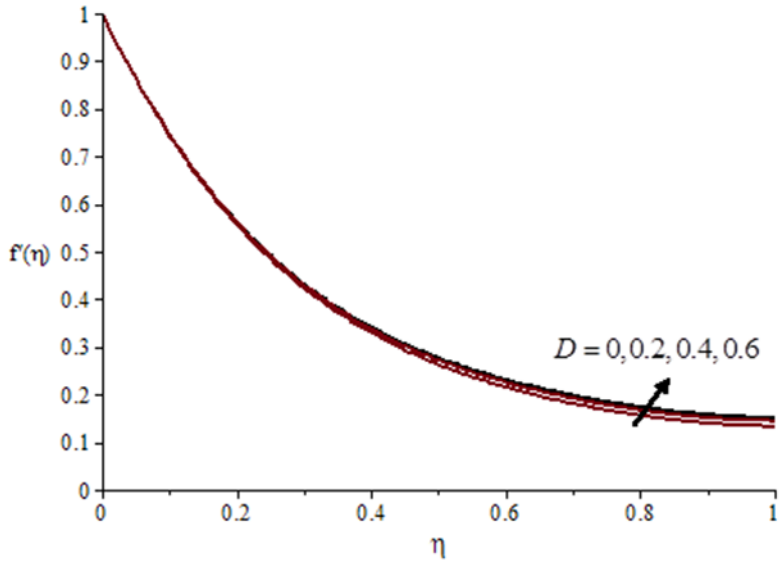

Fig. 2. Velocity profile for different values of D when $S = 0.8$, $Pr = 1$ and $R = 1$.

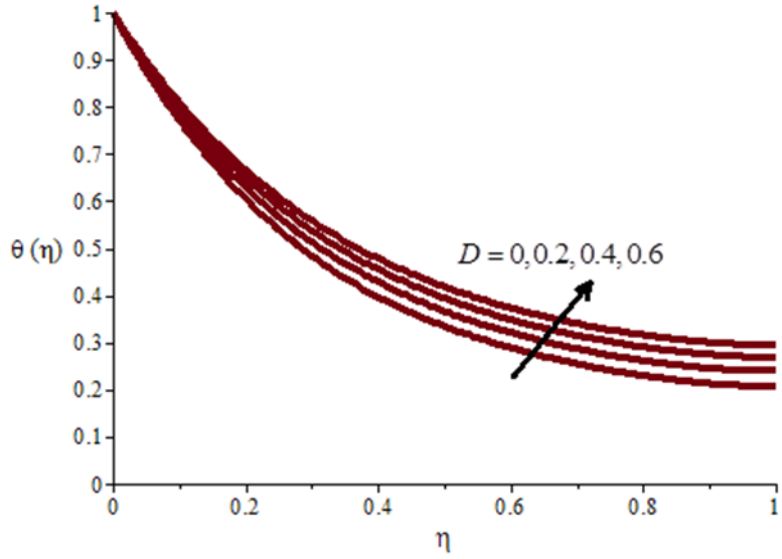

Fig. 3. Temperature profile for different values of D when $S = 0.8$, $Pr = 1$, $R = 1$.

Figure 2 demonstrates the variations of the velocity against η for different values of the Darcy parameter D. It is observed that the velocity decreases as the Darcy parameter increases along the sheet and the reverse is true away from the sheet. Figure 3 shows the dimensionless temperature profile $\theta(\eta)$ for various values of D. It can be seen that the temperature increases with D at each point. This is due to the fact that the porous medium produces a resistive type of force which leads to reduction and increase in the fluid velocity and in the temperature, respectively.

In fig. 4, we can see how the unsteadiness parameter S affects the temperature distribution. As shown in the figure, the temperature rises as the unsteadiness parameter increases. Figure 5 also depicts the effect of the unsteadiness parameter S on the velocity profile. We can observe that the velocity along the surface increases with the unsteadiness parameter S.

The effect of the Prandtl number Pr on the dimensionless temperature profile $\theta(\eta)$ is illustrated in fig. 6. It can be seen that the temperature decreases with the increase of the Prandtl number. This phenomenon is due to the fact that fluids with larger Prandtl numbers possess larger heat capacity, which in turn enhances the heat transfer.

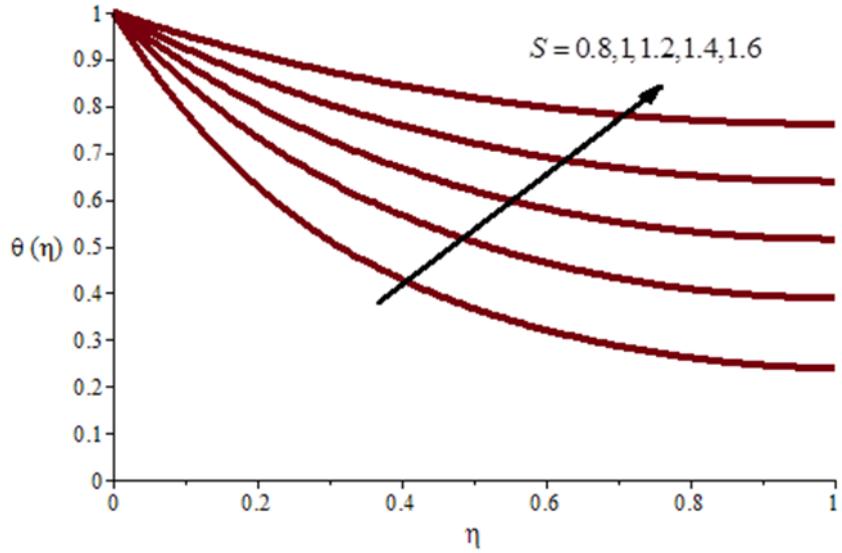

Fig. 4. Temperature profile for different values of S when $D = 0.2$, $Pr = 1$, $R = 1$.

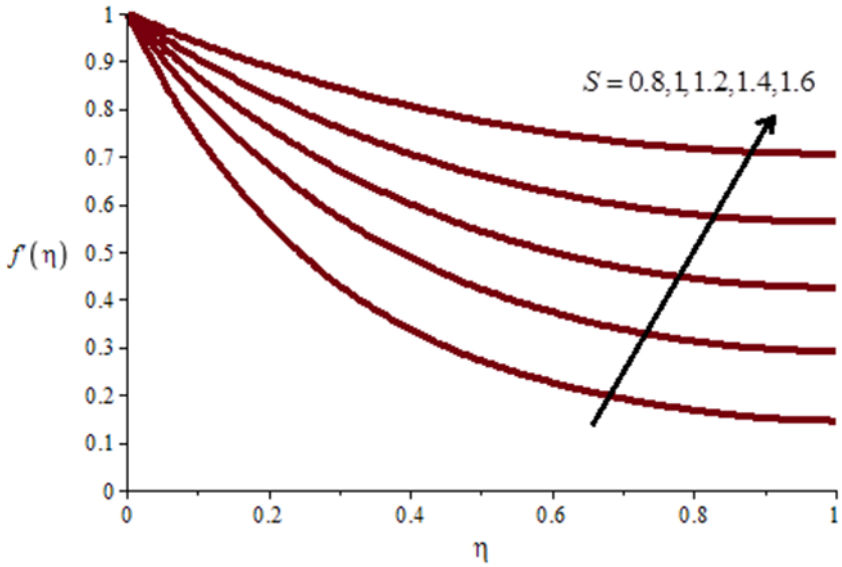

Fig. 5. Velocity profile for different values of S when $D = 0.2$, $Pr = 1$, $R = 1$.

In fig. 7 the effect of the radiation parameter R on the dimensionless temperature $\theta(\eta)$ is displayed. It can be observed that in each point with the increase of the radiation parameter R, the temperature rises. This phenomenon is due to the fact that a higher radiation parameter implies a larger surface heat flux which leads to increase the temperature of the fluid.

5 Conclusions

In this paper, the least-square method is used for solving the problem of the flow and heat transfer in a thin liquid film over an unsteady stretching sheet embedded in a porous medium in the presence of thermal radiation. In order to reduce the partial differential equations describing the problem into a system of ordinary differential equations, the similarity transformation is used. Afterwards, the obtained set of two nonlinear ODE is solved analytically by the

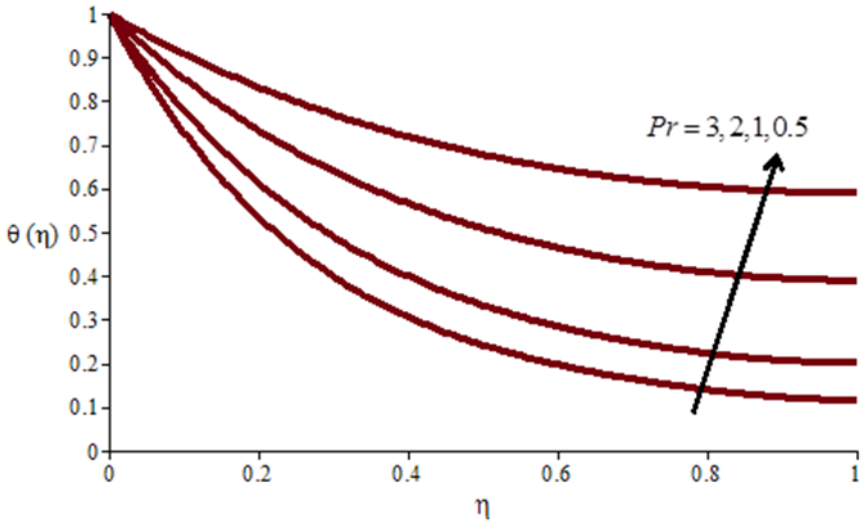

Fig. 6. Temperature profile for different values of Pr when $D = 0.2$, $S = 1$, $R = 1$.

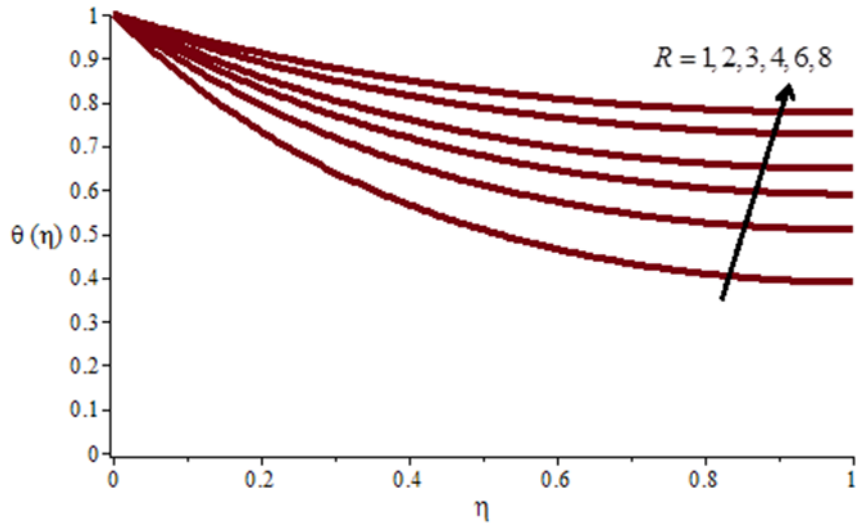

Fig. 7. Temperature profile for different values of R when $D = 0.2$, $S = 1$, $Pr = 1$.

least-square method. From the presented results we can observe that the analytical solution is in excellent agreement with those obtained numerically from the FDM method [26]. Summarizing these results, we can say that the least-square method in its general form gives reasonable calculations, easy to use and can be applied to the differential equations in a general form.

References

1. P. Cheng, W.J. Minkowycz, J. Geophys. Res. **82**, 2040 (1977).
2. P. Cheng, Int. J. Heat Mass Transfer **20**, 807 (1977).
3. G. Ramanaiah, G. Malarvizhi, Int. J. Heat Fluid Flow **12**, 89 (1991).
4. W.B. Hooper, T.S. Chen, B.F. Armaly, Numer. Heat Transfer **25**, 317 (1993).
5. S.D. Wright, D.B. Ingham, I. Pop, Trans. Porous Medium **22**, 181 (1996).
6. K.A. Yih, Int. Commun. Heat Mass Transfer **24**, 1195 (1997).

7. R.S.R. Gorla, H.S. Takhar, Int. J. Numer. Methods Heat Fluid Flow **7**, 596 (1997).
8. K.E. Chin, R. Nazar, N.M. Arifin, I. Pop, Int. Commun. Heat Mass Transfer **34**, 464 (2007).
9. A.M. Rashad, M.A. EL-Hakiem, M.M.M. Abdou, Comp. Math. Appl. **62**, 3140 (2011).
10. L.J. Crane, Z. Angew. Math. Phys. **21**, 645 (1970).
11. L.G. Grubka, K.M. Bobba, J. Heat Transfer **107**, 248 (1985).
12. C.Y. Wang, Z. Angew. Math. Phys. **39**, 177 (1988).
13. K.B. Pavlov, Magn. Gidrodin. **4**, 146 (1974).
14. K.R. Rajagopal, T.Y. Na, A.S. Gupta, Rheol. Acta **23**, 213 (1984).
15. H.I. Andersson, K.H. Bech, B.S. Dandapat, Int. J. Non-Linear Mech. **27**, 929 (1992).
16. S.J. Liao, J. Fluid Mech. **488**, 189 (2003).
17. H.I. Andersson, O.R. Hansen, B. Holmedal, Int. J. Heat Mass Transfer **37**, 659 (1994).
18. C.Y. Wang, Q. Appl. Math. **48**, 601 (1990).
19. H.I. Andersson, J.B. Aarseth, N. Braud, B.S. Dandapat, J. Non-Newtonian Fluid Mech. **62**, 1 (1996).
20. H.I. Andersson, J.B. Aarseth, B.S. Dandapat, Int. J. Heat Mass Transfer **43**, 69 (2000).
21. C.H. Chen, Heat Mass Transfer **39**, 791 (2003).
22. I. Chung Liu, Helge I. Andersson, Int. J. Therm. Sci. **47**, 766 (2008).
23. B.S. Dandapat, B. Santra, H.I. Andersson, Int. J. Heat Mass Transfer **46**, 3009 (2003).
24. C. Wang, Heat Mass Transfer **42**, 759 (2006).
25. N.F.M. Noor, I. Hashim, Int. J. Heat Mass Transfer **53**, 2044 (2010).
26. M.M. Khader, Ahmed M. Megahed, J. King Saud Univ. Eng. Sci. **25**, 29 (2013).
27. Susanta Maity, Int. J. Heat Mass Transfer **70**, 819 (2014).
28. M.N. Ozisik, *Heat conduction*, 2nd edition (John Wiley & Sons Inc., USA, 1993).
29. R.H. Stern, H. Rasmussen, Comput. Biol. Med. **26**, 255 (1996).
30. B. Vaferi, V. Salimi, D. Dehghan Baniani, A. Jahanmiri, S. Khedri, J. Petrol. Sci. Eng. **98-99**, 156 (2012).
31. M. Hatami, A. Hasanpour, D.D. Ganji, Energy Convers. Manage. **74**, 9 (2013).
32. M. Sheikholeslami, M. Hatami, D.D. Ganji, Powder Technol. **246**, 327 (2013).
33. M.N. Bouaziz, A. Aziz, Energy Convers. Manage. **51**, 76 (2010).
34. A. Aziz, M.N. Bouaziz, Energy Convers. Manage. **52**, 2876 (2011).
35. G. Shaoqin, D. Huoyuan, Acta Math. Sci. **28B**, 675 (2008).
36. M. Hatami, D.D. Ganji, Energy Convers. Manage. **76**, 185 (2013).
37. M. Hatami, D.D. Ganji, Energy Convers. Manage. **78**, 347 (2014).
38. Seiyed E. Ghasemi, M. Hatami, A. Kalani Sarokolaie, D.D. Ganji, Physica E **70**, 146 (2015).
39. S.E. Ghasemi , M. Hatami, D.D. Ganji, J. Mech. Sci. Technol. **27**, 3525 (2013).
40. Seiyed E. Ghasemi, M. Hatami, D.D. Ganji, Case Stud. Therm. Eng. **4**, 1 (2014).
41. S.E. Ghasemi, P. Valipour, M. Hatami, D.D. Ganji, J. Cent. South Univ. **21**, 4592 (2014).
42. M. Vatani, S.E. Ghasemi, D.D. Ganji, Proc. Inst. Mech. Eng. Part E: J. Process Mech. Eng. **12**, 0954408914557375 (2014).
43. Seiyed E. Ghasemi, M. Vatani, D.D. Ganji, Particuology (2015) doi:10.1016/j.partic.2014.12.008.
44. S.E. Ghasemi, M. Hatami, GH.R. Mehdizadeh Ahangar, D.D. Ganji, Journal of Electrost. **72**, 47 (2014).
45. A. Raptis, Int. J. Heat Mass Transfer **41**, 2865 (1998).
46. A. Raptis, Int. Commun. Heat Mass Transfer **26**, 889 (1999).